

FLI1 and GATA1 govern *TLN1* transcription: new insights into FLI1-related platelet disorders

Elisa Gabinaud,¹ Laurent Hannouche,¹ Mathilde Veneziano-Broccia,¹ Johannes Van Agthoven,² Justine Suffit,¹ Julien Maurizio,¹ Delphine Potier,³ Dominique Payet-Bornet,³ Delphine Bastelica,¹ Elisa Andersen,¹ Manal Ibrahim-Kosta,¹ Timothée Bigot,¹ Céline Falaise,⁴ Hemostasis Unit of Lille,⁵ Anne Vincenot,⁶ Pierre-Emmanuel Morange,¹ Paul Saultier,^{1,4} Marie-Christine Alessi^{1,4} and Marjorie Poggi¹

¹Aix-Marseille Univ, INSERM, INRAe, C2VN, Marseille, France; ²Structural Biology Program, Division of Nephrology/Department of Medicine, Massachusetts General Hospital and Harvard Medical School, Charlestown, MA, USA; ³Aix-Marseille Univ, CNRS, INSERM, Institut Paoli-Calmettes, CRCM, Marseille, France; ⁴APHM, CHU Timone, French Reference Center on Inherited Platelet Disorders, Marseille, France; ⁵Hemostasis Unit, Hospital University Center Lille, Lille, France and ⁶CHU Robert Debré, National Reference Center for Inherited Platelet Disorders and Biological Hematology Service, AP-HP, Paris, France

Correspondence: M. Poggi
marjorie.poggi@univ-amu.fr

Received: August 1, 2024.
Accepted: December 16, 2024.
Early view: January 2, 2025.

<https://doi.org/10.3324/haematol.2024.286372>

©2025 Ferrata Storti Foundation
Published under a CC BY-NC license



SUPPLEMENTARY METHODS

Analysis of single-cell RNA sequencing data

This was conducted as previously described¹. For both scRNA-seq experiments (day 5 and day 11), mRNA library reads were aligned to the human hg38 reference genome (GRCh38-2020-A) and quantified using the cellranger count toolkit (version 5.0.0). Cell hashing antibodies were quantified using CITE-seq-Count (version 1.4.3) with default parameters. The resulting mRNA and hashtag oligo (HTO) matrices were imported into R (version 4.1.2) in order to perform downstream analyses using the Seurat package (version 4.3.0). Cells were demultiplexed using the *HTODemux* and *MULTISeqDemux* functions except for “set5” where HTO staining was not efficient. In addition, specific single nucleotide variants were identified for each sample using the Soupcorell method (version 2.0) to rescue unassigned cells and improve demultiplexing. Associations were also confirmed between cells and samples while examining the mutation with the Integrative Genomics Viewer (IGV) and sex genes (XIST and YBX). Cell multiplets and negatives were removed from the filtered cellranger barcode matrix. Quality controls included filtering out low quality cells (i.e. cells with a feature count < 200 and with less than a 10% threshold of mitochondrial gene expression where the threshold ranged from 8 to 10% and was calculated using the `scater::isOutlier` function) and genes expressed in few cells (e.g., genes expressed in less than 3 cells). Samples from the two time points (days 5 and 11) were merged using the Seurat merge function. The merge quality and absence of batch effects were subsequently assessed by overlapping several cell groups at both time points. After normalization and regression scaling based on cell cycle genes, two-dimensional reduction was performed. The merged object was reduced using principal component analysis (PCA) (`Seurat::RunPCA`) with the 1000 most variable genes (`Seurat::FindVariableFeatures`). The PCA reduction was used to generate a UMAP with the first 10 components (`Seurat::RunUMAP`). The nearest-neighbor graph (k-nn) was generated using the `Seurat::FindNeighbors` function with a k parameter equal to 12 and the first 8 components merging datasets. Cell clusters were defined using the `Seurat::FindClusters` function with the Louvain algorithm (resolution of 0.4). This Seurat analysis was split between controls and FLI1 patient and each subset object was individually processed as previously mentioned. Based on our previously published hematopoietic gene signature¹ and the top 20 cluster differentially expressed genes, cell type-specific signatures were adapted, scored for controls and patient independently and assigned to each cluster. These assignments were transferred onto the merged object and differential gene expression analysis was performed for each cell type (controls vs. FLI1 patient) with a log fold-change threshold equal to 0 and using the “bimod” test (Likelihood-ratio test for single cell gene expression).² Differentially expressed genes with

a p-value < 0.05 and either average log2 fold change > 0 or average log2 fold change < 0 were filtered. An enrichment analysis was performed on five different databases (Transfac and Jaspar, KEGG 2019, GO Biological process 2018, Reactome 2016 and Transcription factor PPI) and summarized in bubble plots. To infer gene regulatory networks implicated in FLI1-related transcriptome dysregulation, we used the SCENIC method using a cellranger-filtered raw unique molecular identifier (UMI) matrix. All statistical tests comparing patients to controls were performed using the Wilcoxon test, with a p-value < 0.05 considered statistically significant.

Data and code availability

All the sequencing data has been deposited in NCBI's Gene Expression Omnibus and are accessible through GEO series accession number (GSE273210). The human transcriptome reference used in our study is available on 10X Genomics website (<https://cf.10xgenomics.com/supp/cell-exp/refdata-gex-GRCh38-2020-A.tar.gz>) or Zenodo (<https://zenodo.org/uploads/12759766>). Docker images and detailed scripts used for preprocessing and further analysis are available at Zenodo (<https://zenodo.org/uploads/12759766>) and GitHub (https://github.com/poggiteam/FLI1_2021), respectively.

Light transmission platelet aggregation

Citrated blood was collected by antecubital venipuncture into Becton-Dickinson vacutainer tubes containing 0.105 mol/L trisodium citrate. Platelet-rich plasma (PRP) was prepared in accordance with the ISTH recommendations.^{3,4} Platelet aggregation was assessed by measuring light transmission through the stirred suspensions of PRP for 5 min using an AACT 4004 aggregometer. Platelet aggregation was triggered by adding 2.5 and 5 μ M adenosine diphosphate (ADP; Helena Laboratories) and 2 μ g/ml collagen (Bio/Data Corporation).

Evaluation of platelet granules

Electron microscopy was performed as previously described.⁵ For the intraplatelet serotonin measurement, the PRP was subjected to two freeze/thaw cycles. An automated platelet count of the PRP was performed prior to the serotonin measurement in order to normalize the serotonin level to the platelet count; results were expressed as μ g/ 10^9 platelets. The plasma serotonin level was considered negligible as compared to the intraplatelet serotonin content. Serotonin was quantified using high-performance liquid chromatography (HPLC) (Dionex,

Thermo Scientific©) coupled with electrochemical detection (Precision Instruments©, Model 105).

Platelet ATP/ADP levels were assessed using HPLC on an anion exchange column. Assays have been performed at the Hemostasis Laboratory-EFS-Strasbourg-France.

The Mepacrine test was performed as previously described.⁵ Briefly, PRP count was adjusted to 10 platelets x 10⁹/L. Platelet mepacrine uptake was assessed after 30 minutes incubation at 37°C without or with mepacrine (Quinacrine dihydrochloride, Cas number 69-05-6, Sigma) at 1 and 2 µmol/L final concentration.

MSR cell culture

GripTite™ 293 cells (a genetically engineered Human Embryonic Kidney (HEK 293) cell line that expresses the human macrophage scavenger receptor, Thermo Fisher Scientific) were cultured in DMEM supplemented with 10% fetal bovine serum, 100 U/mL penicillin, 0.1 mg/mL streptomycin, 1% GlutaMAX™ and 1% non-essential amino acids.

Luciferase reporter assay

Transcriptional regulatory properties of WT FLI1 and FLI1 variants were analyzed using the E743tk80Luc plasmid containing the luciferase gene driven by an enhancer cassette comprised of three tandem copies of the Ets *Binding Site (EBS) inserted 5' of the herpes simplex virus thymidine kinase promoter*, as previously described⁶. Directed mutagenesis of the human expression plasmid pCMV3-FLI1-HA (Sino Biological Inc.) was performed using the GeneArt Site-directed Mutagenesis System kit (Thermo Fischer Scientific) according to the *manufacturer's instructions*. GripTite™ 293 MSR Cells, a genetically engineered Human Embryonic Kidney 293 cell line (Thermo Fisher Scientific), were transfected using PolyJet In Vitro DNA Transfection Reagent (SignaGen Laboratories). The transfection included the reporter gene constructs (150 ng), the expression plasmid (330 ng) and SV40-driven luciferase plasmid (pGL473-hRLuc) (10 ng) for normalization of transfection efficiency.

The identified regulatory regions in the *TLN1* gene were cloned into a pGL3 vector and confirmed using Sanger DNA sequencing (Proteogenix). To investigate cell-type dependence, the HEL (human erythroleukemia) hematopoietic and GripTite 293 MSR cell lines were used. Transfections with expression plasmids (*FLI1*, *GATA1*, *RUNX1*, and *SCL*) and the pGL3 vector along with the pGL473-hRLuc for normalization, were carried out using PolyJet In Vitro DNA Transfection Reagent. The cells were harvested and lysed 48 hours post-transfection and Firefly and Renilla luciferase activities were measured consecutively using the reporter gene

detection kit (Yelen) with an EnSight™ Multimode Microplate Reader (PerkinElmer) according to the manufacturer's instructions.

Western blot assay

To isolate nuclear and cytoplasmic subcellular fractions from protein lysates, MSR cells were lysed 48h after transfection (PolyJet In Vitro DNA Transfection Reagent, SignaGen Laboratories). Fractionation was performed using the NE-PER Nuclear and Cytoplasmic Extraction Reagent (Pierce). Total platelet proteins from washed platelets and proteins from the subcellular fractions were separated on NuPAGE gels with MES SDS running buffer (Thermo Fisher Scientific) and transferred onto a polyvinylidene fluoride membrane. Membranes were blocked and labeled overnight with the following primary antibodies: rabbit anti-FLI1 (Santa Cruz Biotechnology; ref: sc-356), rabbit anti-HA (Santa-Cruz Biotechnology; sc-805), rabbit anti-MYH10 (Santa Cruz Biotechnology; sc-376942), rabbit anti-LAMIN-B1 (sc-374015), mouse anti-Talin (sc-365875), rabbit anti-MYH9 (Protein tech; 11128-1-AP), mouse anti-FlnA (Santa Cruz Biotechnology; sc17749), and mouse anti-GAPDH (Millipore; MAB374). Horseradish peroxidase-conjugated secondary antibodies (Bio-Rad) were used, and chemiluminescence signals were obtained using Pierce ECL Western Blotting Substrate (Thermo Fisher Scientific; 32106) or Ultra High Sensitivity ECL kit substrate (MedChem Express; HY-K1005). Images were captured using a CCD Imager ImageQuant LAS 4000 (GE Healthcare) and quantified using ImageJ software (National Institutes of Health, Bethesda, Maryland).

H9C2 cell culture

H9C2 cells (cell line derived from embryonic BD1X rat heart tissue; ATCC CRL-1446) were cultured in DMEM supplemented with 10% fetal bovine serum, 100 U/mL penicillin, 0.1 mg/mL streptomycin, and 1% GlutaMAX™.

Epifluorescence microscopy

MSR cells or H9C2 cells were fixed in 1% paraformaldehyde for 15 minutes at room temperature 48 hours after transfection. After washing, cells were permeabilized with 0.3% Triton X-100 in PBS for 10 minutes, blocked for 30 minutes using 1% BSA-PBS and incubated overnight with rabbit anti-HA antibody (Santa Cruz Biotechnology; sc-805). Subsequently, cells were incubated with anti-rabbit Alexa 488-labeled secondary antibody (Abcam; ab150077) and then with phalloidin rhodamine (Cytoskeleton, Inc. PHDR1) for 30 minutes. After washing

steps, slides were mounted with DAPI-Fluoromount for examination using an AXIO Imager M1 microscope (Carl Zeiss, Germany).

Protein stability assay

GripTite™ 293 MSR cells were transfected with pCMV3-FLI1-HA (WT and FLI1 variants). After 48 hours cells were treated with 50 μ g/mL cycloheximide (CHX) (Sigma; C-6255) to inhibit protein synthesis. Cells were harvested at different time points (0, 5.5, and 9 hours) and processed for immunoblotting with anti-HA and anti-GAPDH antibodies.

Structural model of FLI1 interactions

Prediction of affinity changes. The impact of mutations on the FLI1-DNA interaction was analyzed through $\Delta\Delta G$ predictions on the structure of FLI1 in complex with a 10-mer of double-stranded DNA ACCGGAAGTG (PDB code 5e81) using the protein-DNA SAMPDI-3D Web server (compbio.clemson.edu/SAMPDI-3D/#started). SAMPDI-3D applies $\Delta\Delta G$ values derived from physico-chemical and structural properties of the mutated protein-DNA site to a gradient lifting machine learning algorithm based on a large, high-quality dataset.⁷ *MutaBind2 was utilized to assess changes in binding affinity ($\Delta\Delta G$) caused by FLI1 mutations (G307R, R337Q, R340C, and K345E) on the FLI1 homodimer within the FLI1/DNA structure (PDB code 5e8).* *MutaBind2 calculates $\Delta\Delta G$ values based on side-chain optimization and multiple rounds of energy minimization algorithms incorporating molecular mechanics and static force fields.*⁸

Fibrinogen binding to platelets

One hundred microliters of RPMI-diluted platelets at a concentration of 6×10^3 platelets/ μ L were incubated with 10 μ L of a rabbit anti-fibrinogen conjugated to FITC (Thermo Fisher Scientific RB-1924-R2) and 90 μ L of PBS, with or without TRAP6 (10 μ M), for 15 minutes at room temperature. Fibrinogen binding was measured using flow cytometry. Results are expressed as mean fluorescence intensity.

MEG01 cell culture

MEG01 cells were obtained from Sigma and cultured in RPMI-1640 supplemented with 10% fetal bovine serum, 100 U/mL penicillin, 0.1 mg/mL streptomycin, and 1% GlutaMAX™. For siRNA treatments, 250,000 cells underwent 2 sequential transfections with 10 pmol of control siRNA (Santa Cruz; 37007) or 10 pmol of FLI1 siRNA (Santa Cruz; 35384).

Transfections were performed on days 1 and 4 using the PepMute™ Plus siRNA Transfection Reagent (SignaGen Laboratories; SL10057). Cells were lysed with RIPA on day 7.

For transduction, *GATA1* and *FLI1* DNA were subcloned into a lentiviral vector pRRLSIN-MND-IRES2-ZsGreen-WPRE, and lentiviral particles were prepared by VectUb platform at Bordeaux University. MEG01 cells were transduced with a multiplicity of infection (MOI) of 7.5, to overexpress FLI1 and with a MOI of 25 to overexpress GATA1, then lysed with RIPA after 2 weeks.

Electrophoretic mobility shift assay

Nuclear extracts were prepared from MSR cells transfected with either the empty vector, WT *FLI1*, or *GATA1*, using the Pierce NE-PER Nuclear and Cytoplasmic Extraction Kit, according to the manufacturer's instructions. *Cell extracts were stored at -80°C until use.* The oligonucleotides used in EMSA analysis were synthesized and labeled with streptavidin by Proteogenic as follows: intronic BS3 of *TLN1*, 5'-TAT CCG CTT GTG TCC CAG CTG GAC AGA CCT GGC TAT GGG GTT GCT GAC CAT GAA AGA ATG AGG GCT GGG CTG GTG GAT CCG AGA AGC TGG AGG AGT CTG TGG AGC CAA GAA GCA GGA CTG AAA GGA CCC TTC ACA CTA AGC TGA AAC TGC ATG TCT CCC CCC ATT TCC TCT GGA CAC TTA GAC ACC CCC TTC CTC CTC AAG CAC GGA AGC CTC TGG TGA GAC CCC GAT AAG GGA GCT GAG TCA TGC CTA CCC TTA CTC CCC AGC TGG TCC AGA GTG GAT ATT CAC ACA GCT ACA AGA GGG TGT GTG GAC GCG AAG AAC TGA TCA GTG AAT TGT GGG T-3'. *The labeled oligonucleotides were then incubated with* nuclear extracts in the binding buffer (from Light Shift kit, Thermo Fisher Scientific 20148X). Binding reactions were performed in 20 µl containing 1 fmol oligonucleotides, 1X binding buffer, 1µg of poly (dl-dC), 50% glycerol, 1% NP40, 100 mM MgCl₂, 1X charge buffer (Thermo Fisher Scientific, 20148X). The samples were then run on a native 6% polyacrylamide gel. The contents of the gel were then transferred to a nylon membrane (Thermo Fisher Scientific, 77015) and crosslinked to the membrane using a UV crosslinker. Membranes were blocked and then visualized using the reagents provided in the Light Shift kit.

Protein interaction studies

Detection of FLI1 and GATA1 interaction in MSR cells was performed using the Duolink® In situ Detection Reagents (Sigma-Aldrich, St. Louis, MO, USA) according to the manufacturer's instructions. Briefly, MSR cells were first incubated with two primary antibodies that recognize the target proteins, rabbit anti-HA (Thermo Fisher Scientific, 71-5500) and mouse anti-c-MYC (Santa Cruz, sc-40) antibodies, and then incubated with a pair of proximity ligation assay (PLA)

probes consisting of species-specific secondary antibodies (anti-rabbit and anti-mouse) conjugated to complementary oligonucleotides. In the presence of hybridization solution and ligase, the oligonucleotides form a circle when the proteins are in close proximity. Finally, the polymerase and nucleotides participate in the formation of rolling circle amplification, which is visualized as red fluorescence. After washing steps, slides were mounted with DAPI-Fluoromount for examination using an AXIO Imager M1 microscope (Carl Zeiss, Germany).

REFERENCES

1. Bigot T, Gabinaud E, Hannouche L, et al. Single-cell analysis of megakaryopoiesis in peripheral CD34+ cells: insights into ETV6-related thrombocytopenia. *J Thromb Haemost.* 2023;S1538-7836(23)00321–5.
2. McDavid A, Finak G, Chattopadhyay PK, et al. Data exploration, quality control and testing in single-cell qPCR-based gene expression experiments. *Bioinformatics.* 2013;29(4):461–467.
3. Cattaneo M, Cerletti C, Harrison P, et al. Recommendations for the standardization of light transmission aggregometry: a consensus of the working party from the platelet physiology subcommittee of SSC/ISTH. *J Thromb Haemost.* 2013;11(6):1183–1189.
4. Gresele P, Subcommittee on Platelet Physiology of the International Society on Thrombosis and Hemostasis. Diagnosis of inherited platelet function disorders: guidance from the SSC of the ISTH. *J Thromb Haemost.* 2015;13(2):314–322.
5. Saultier P, Vidal L, Canault M, et al. Macrothrombocytopenia and dense granule deficiency associated with FLI1 variants: ultrastructural and pathogenic features. *Haematologica.* 2017;102(6):1006–1016.
6. Poggi M, Canault M, Favier M, et al. Germline variants in ETV6 underlie reduced platelet formation, platelet dysfunction and increased levels of circulating CD34+ progenitors. *Haematologica.* 2017;102(2):282–294.
7. Li G, Panday SK, Peng Y, Alexov E. SAMPDI-3D: predicting the effects of protein and DNA mutations on protein–DNA interactions. *Bioinformatics.* 2021;37(21):3760–3765.
8. Zhang N, Chen Y, Lu H, et al. MutaBind2: Predicting the Impacts of Single and Multiple Mutations on Protein-Protein Interactions. *iScience.* 2020;23(3):100939.

SUPPLEMENTARY FIGURES

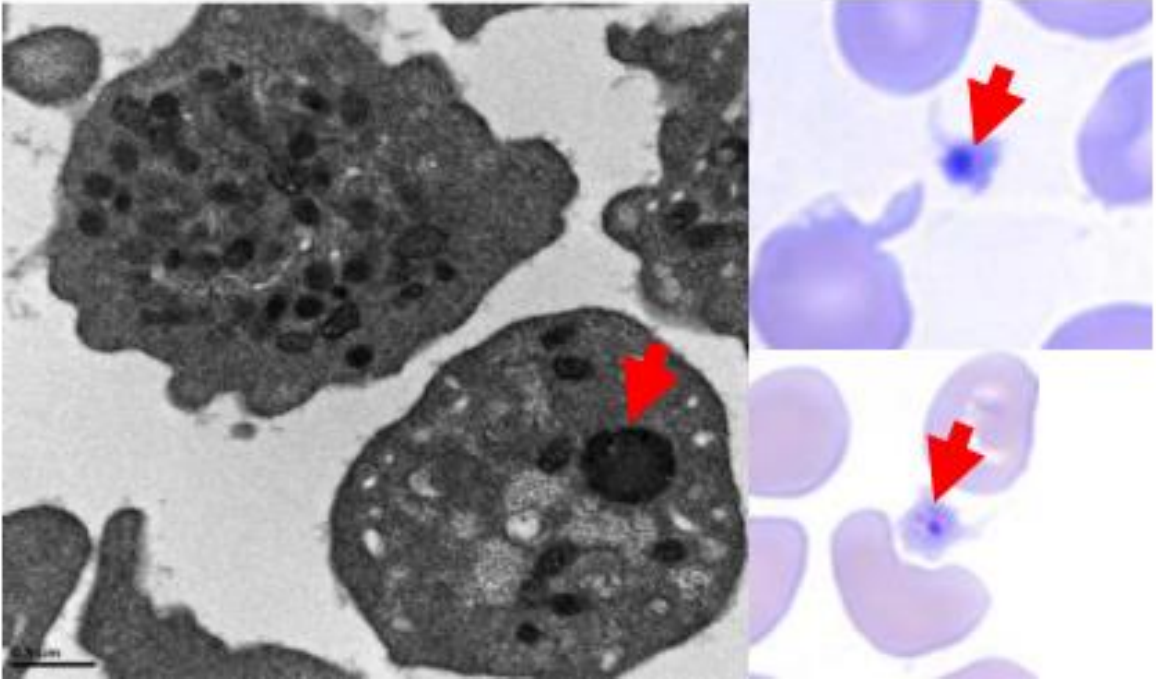


Figure S1: Giant alpha granules in patient platelets. Left: Electron microscopy image of platelets from the patient carrying the R340C variant; scale bar, 0.5 μm . Right: Blood smears showing platelets from the patient with the G307R variant. Red arrows indicate giant alpha granules.

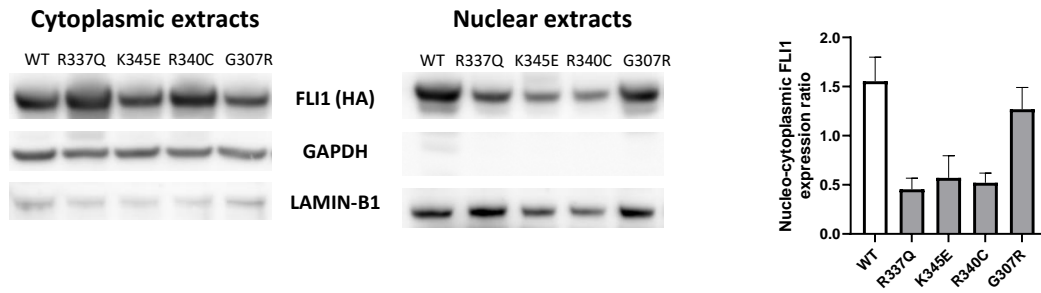


Figure S2: Western blot analysis of WT FLI1 and FLI1 variant subcellular localization. MSR cells were transfected with WT *FLI1* or *FLI1* variant constructs. LAMIN-B1 and GAPDH expression levels were used as nuclear and cytoplasmic markers, respectively. Data are represented as the mean \pm SEM of two independent experiments.

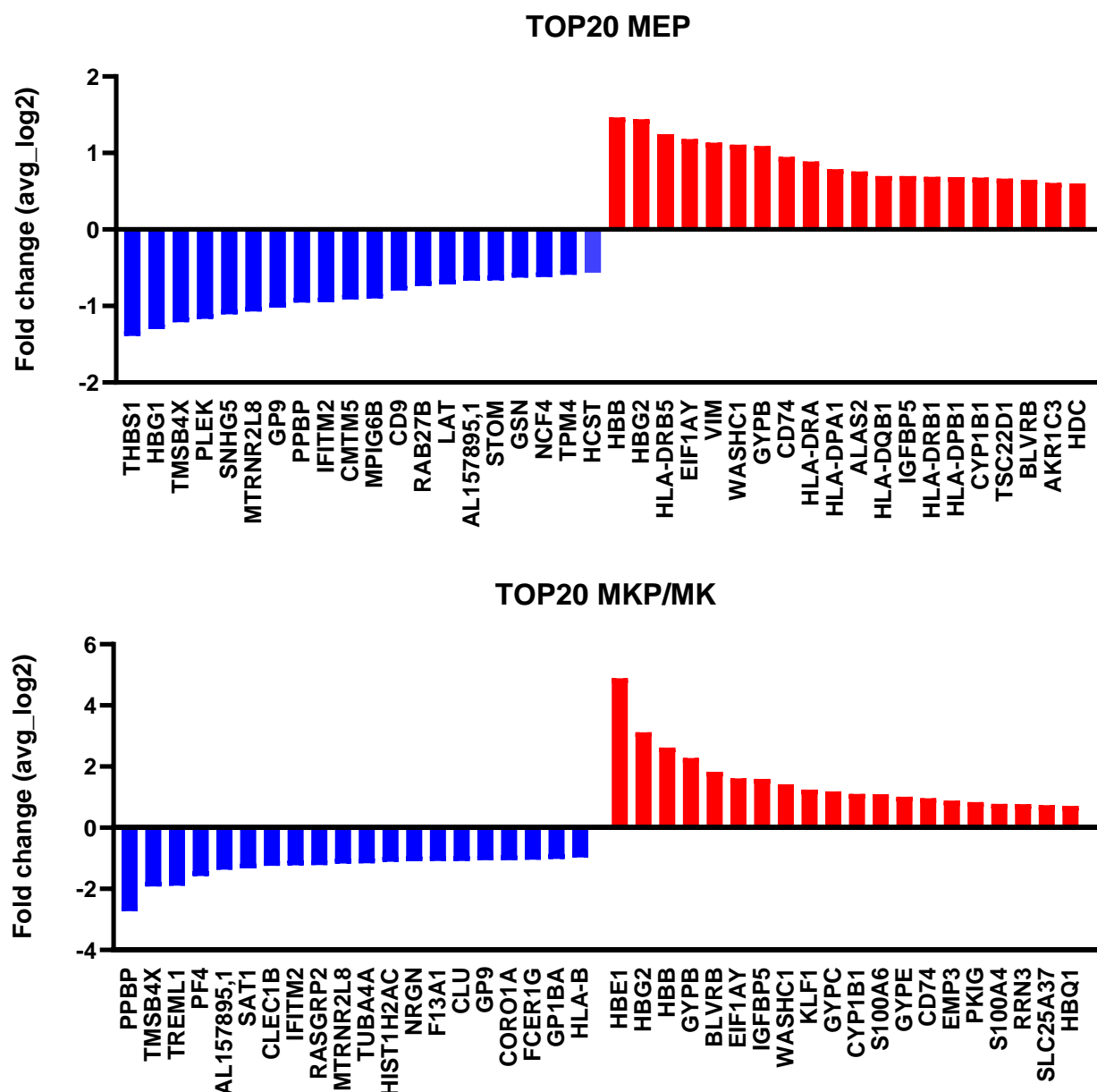


Figure S4: The top 20 differentially expressed genes in patient MEPs and MKP/MKs. Downregulated (depicted in blue) and upregulated genes (depicted in red) in FLI1-mutated MEP and MKP-MK cells compared with control cells ($p < 0.05$) and classified according to log2 fold change.

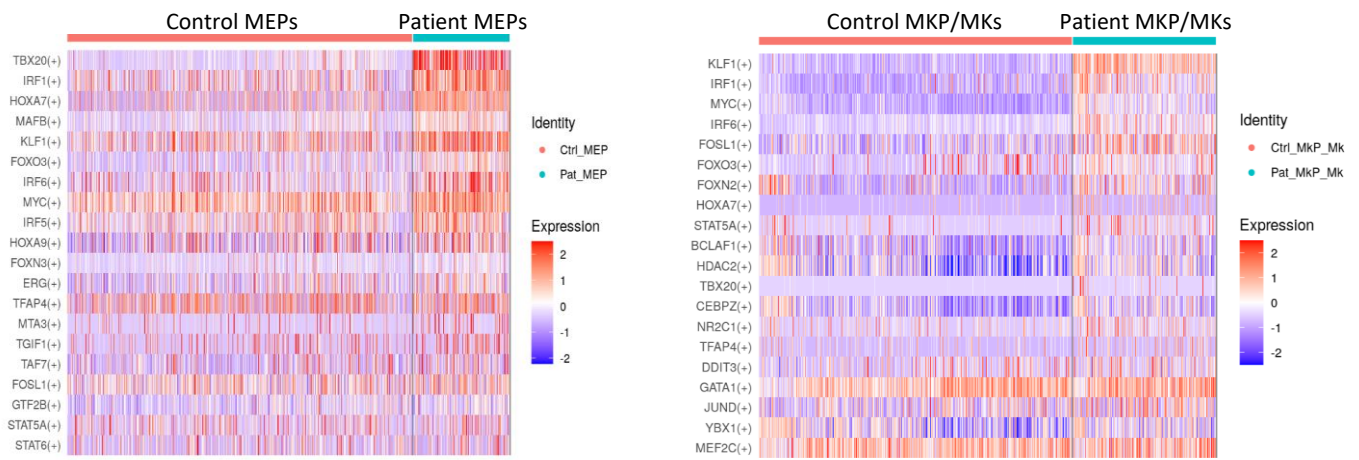


Figure S5: Heatmap showing the top 20 differentially active regulons (patient vs controls). Differentially active regulons in MEPs are displayed on the left, while those for MKP/MKs are shown on the right. The color gradient corresponds to the scaled regulon activity.

Enrichment analysis of KEGG biological process upregulated in patient cells

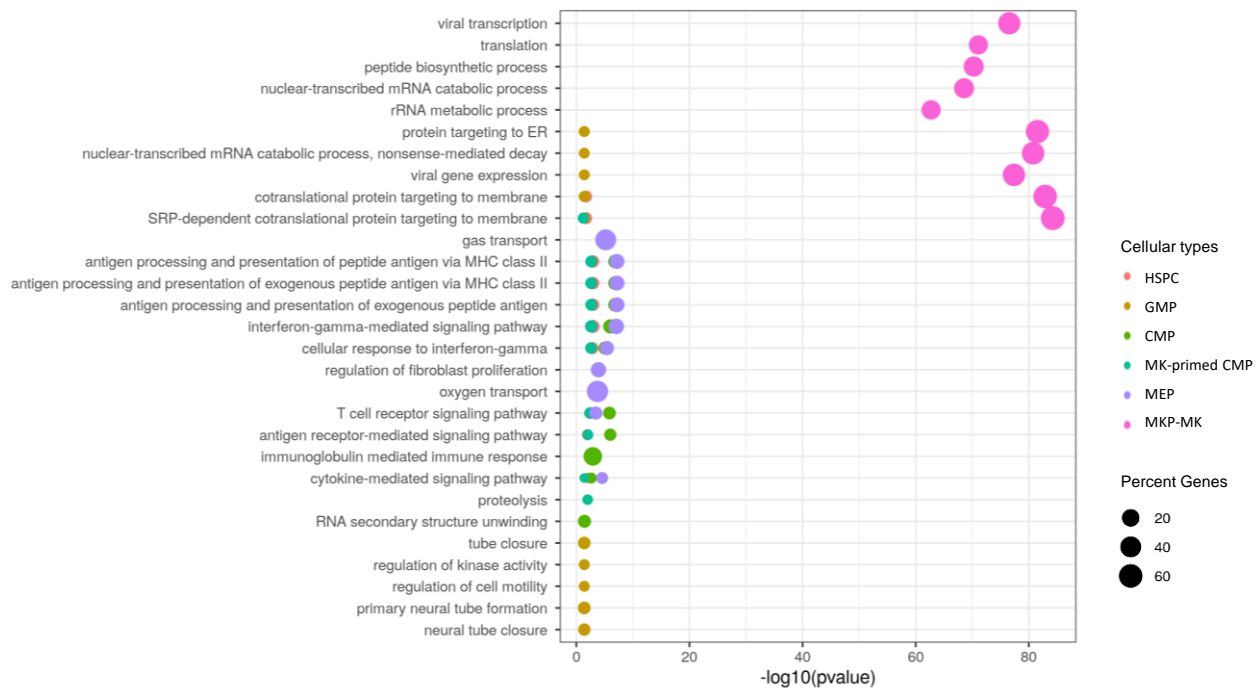


Figure S6: Bubble plot depicting the top upregulated enriched KEGG biological pathways based on differentially expressed genes by cell type. KEGG biological pathways are classified by p-values. Dot sizes reflect the ratio of genes enriched in this pathway to the total number of genes in the pathway. Bubbles are color-coded according to cell type (HSPC, CMP, MK-primed CMP, GMP, MEP, and MKP/MK).

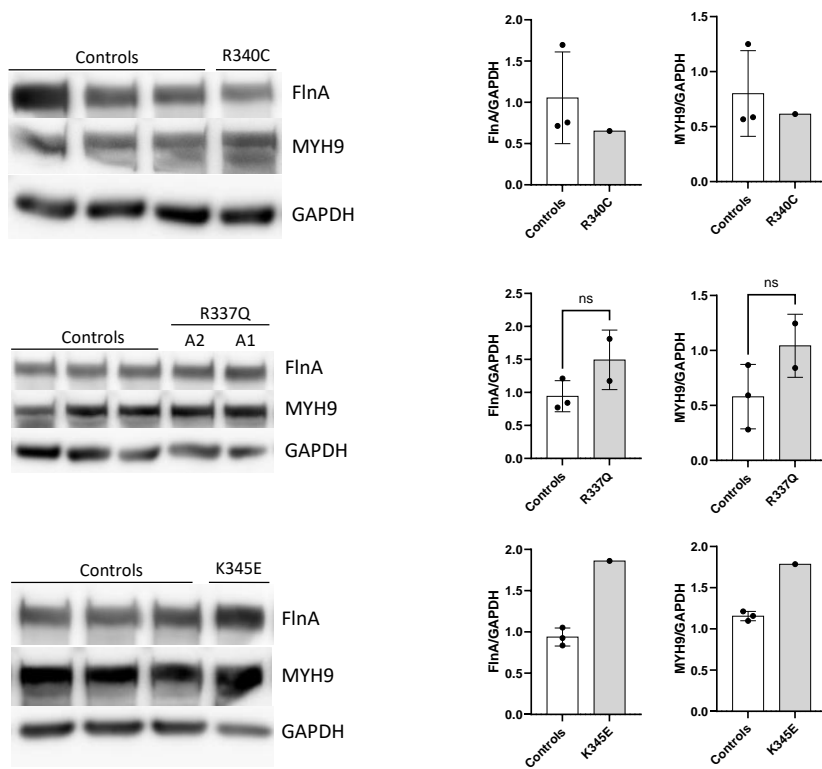
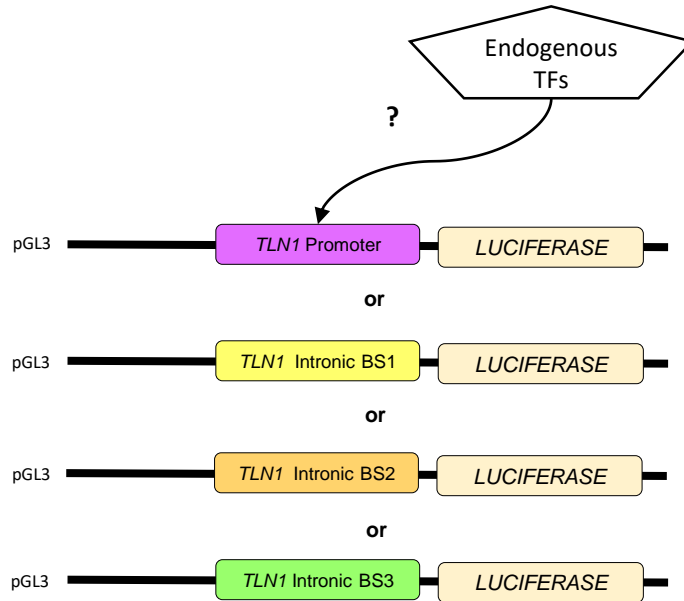


Figure S7: Western blot analysis of FlnA and MYH9 expression in washed platelets from controls and FLI1-variant carriers. GAPDH was used as a protein loading control. Each patient was compared with age- and sex-matched control subjects. For each patient and matched controls, blood samples were collected at the same time and processed in parallel to avoid any bias. Quantification of band intensity is shown on the right.

A

HEL cells



B

MSR cells

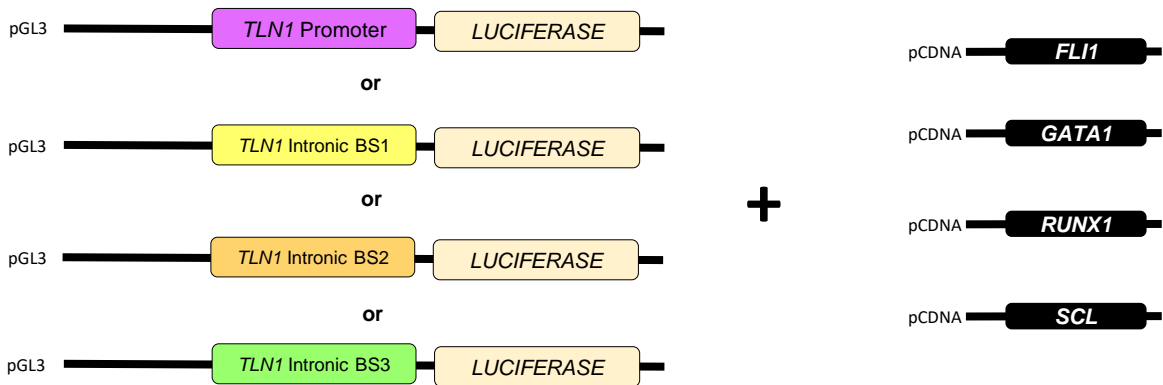
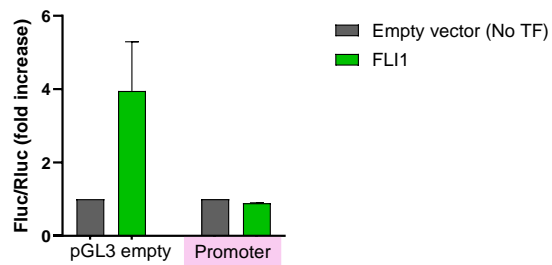
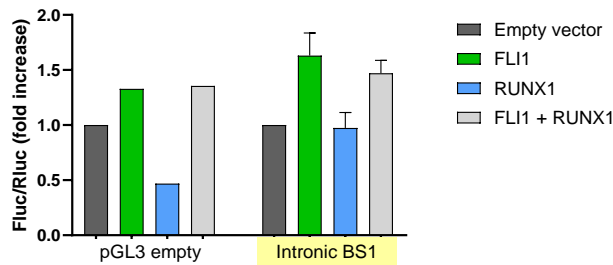


Figure S8: Experimental design of the luciferase reporter assays. Luciferase assays were performed in HEL (A) and MSR (B) cells. Co-transfections of pGL3 reporter vectors with pCDNA vectors were performed according to the ChIP-seq results. TFs: transcription factors; BS: binding site.

A



B



C

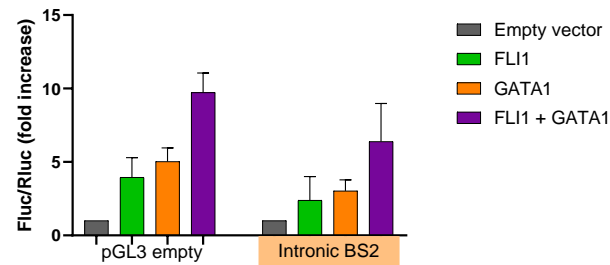


Figure S9: Test of the functionality of *TLN1* regions bound by FLI1. Luciferase reporter assays were performed in MSR cells transfected with DNA sequences corresponding to the promoter (A), intronic binding site 1 (B), and intronic binding site 2 (C) of *TLN1*, along with transcription factors that have binding sites in these sequences based on ChIP-seq analysis. TF: transcription factor; BS: binding site.

SUPPLEMENTARY TABLES

Table S1: Platelet phenotyping in patient C carrying the FLI1 variant R340C.

	Platelet count (x10 ⁹ /l)	MPV (fl)	Platelet aggregation maximal intensity (%)			ADP (nmol/10 ⁸ plt)	ATP (nmol/10 ⁸ plt)	ATP/ADP	PRP serotonin levels (µg/10 ⁹ plt)	Mepacrine uptake (MFI)	CD63 (MFI) TRAP6 50 µM
			ADP	Coll*	AA*						
Reference ranges ^a	150-400	8-12	2 µM : 78-95 5 µM : 76-95	85-96	86-96	1.7-3.7	3.5-5.9	1.2-2.4	0.3-1.2	1 µM : 0.66-0.85 2 µM : 0.81-1	1.3-4.23
Patient C	222	11.2	2 µM : 35 5 µM : 60	64	90	0.9	4	4.45	0.15	1 µM : 0.38 2 µM : 0.49	0.93-1.02

MPV: mean platelet volume (measured by optical method using ADVIA, 120, Siemens). ^aThe reference ranges were defined as the [minimum-maximum] interval of values obtained from healthy individuals in our laboratory in Marseille. *The collagen and arachidonic acid aggregation assays were performed using agonist concentrations of 2 µg/mL and 0.3 mg/mL, respectively. PLT: platelet; PRP: platelet-rich plasma; ADP: adenosine diphosphate; Coll: collagen; AA: arachidonic acid; ATP: adenosine triphosphate; TRAP: thrombin receptor-activating peptide.

Table S2: Platelet phenotyping in patient D carrying the FLI1 variant G307R.

	Platelet count (x10 ⁹ /l)	MPV (fl)	Platelet aggregation maximal intensity (%)			ADP (nmol/10 ⁸ plt)	ATP (nmol/10 ⁸ plt)	ATP/ADP	PRP serotonin levels (µg/10 ⁹ plt)
			ADP	Coll	AA**				
Reference Ranges ^a	150-400	8-12	2 µM : >28 10 µM : >59	1.25 µg/ml : > 75 5 µg/ml : > 78	> 74	1.7-3.7	3,5-5.9	1.2-2.4	0.3-1.2
Patient D	83-147	13.3	2 µM : 65 10 µM : 85	1.25 µg/ml : 75 5 µg/ml : 81	70	NA	0	-	0.087

**The arachidonic acid aggregation assay was performed using 1 mM AA. ^aThe reference ranges were obtained from healthy individuals at the CHU de Lille, where the patient carrying the G307R variant was characterized. NA: not available.

Table S3: Impact of FLI1 variations on FLI1 DNA-binding domain/DNA interface.

Variation	$\Delta\Delta G$ (kcal/mol)	Type	Effect
G307R	-0.09	Stabilizing	Non-disruptive
R337Q	0.98	Destabilizing	Non-disruptive
R340C	1.49	Destabilizing	Disruptive
K345E	1.48	Destabilizing	Disruptive

Table S4: Impact of FLI1 variations on FLI1 homodimerization.

Variation (FLI1/FLI1)	Interface?	$\Delta\Delta G$ (kcal/mol)	Deleterious?
G307R/G307R	Yes	3.59	Yes
R337Q/R337Q	No	0.27	No
R340C/R340C	No	0.21	No
K345E/K345E	No	0.16	No